Very Rapid, Ionic Strength-Dependent Association and Folding of a Heterodimeric Leucine Zipper†

Hans Wendt,‡,§,|| Lukas Leder,‡,||,⊥ Harri Härmä,‡,▽ Ilian Jelesarov,‡ Antonio Baici,# and Hans Rudolf Bosshard*,‡

Biochemisches Institut der Universität Zürich, Winterthurerstrasse 190, CH-8057 Zürich, Switzerland, and Rheumaklinik, Universitätsspital, CH-8091 Zürich, Switzerland

Received July 9, 1996; Revised Manuscript Received September 29, 1996⊗

ABSTRACT: Leucine zippers (coiled coils) are dimerization motifs found in several DNA-binding transcription factors. A parallel leucine zipper composed of the acidic chain X_1-EYQALEKEVAQLEAENX$_2$-ALEKEVAQLEHEG-amide and the basic chain X_1-EYQALKKKVAQLKAKNX$_2$ALKKKVAQLKHKG-amide was designed to study the kinetics of folding of a heterodimeric leucine zipper and to investigate the role of electrostatic attraction between oppositely charged peptide chains to the folding reaction. Each peptide alone did not form a leucine zipper at ionic strength (μ) <1 M because of electrostatic repulsion between like charges in a homodimer. Therefore, the formation of the heterodimeric leucine zipper could be investigated by simple mixing of acidic and basic chains. To monitor folding, a fluorescent label was located either at the N-terminus (X_1 = fluorescein-GGG, X_2 = Q) or in the center of the coiled coil (X_1 = acetyl, X_2 = W). Folding could be described by a simple two-state reaction involving the disordered monomers and the folded heterodimer. The same bimolecular rate constant (k_{on}) was observed independent of the location of the fluorescent label, indicating that both fluorescence probes monitored the same reaction. Lowering of the ionic strength increased k_{on} from 4×10^6 M^{-1} s^{-1} (μ = 525 mM) to about 5×10^7 M^{-1} s^{-1} (μ = 74 mM). When extrapolated to $\mu = 0$, k_{on} was $\sim 10^9$ M^{-1} s^{-1}, which is near the diffusion limit. In contrast, the rate of dissociation depended very weakly on ionic strength; k_{off} decreased only by about 2-fold when μ was lowered from 525 to 74 mM. Equilibrium association constants (K_a) of the heterodimeric zippers measured directly and calculated from kinetic constants ($K_a = k_{on}/k_{off}$) were in good agreement. The observed two-state mechanism, the strong dependence on ionic strength of k_{on} but not of k_{off}, and the nearly diffusion-limited association rate at very low ionic strength point to a folding pathway in which the formation of an electrostatically stabilized dimeric intermediate may be rate-limiting and the subsequent folding to the final dimer is very rapid and follows a "down-hill" free energy landscape. The small increase of k_{off} at increasing ionic strength indicates a minor contribution of electrostatics to the stability of the folded leucine zipper.

When oligomeric proteins are formed, the folding of individual subunits and their assembly to higher order, quaternary structures are coupled processes. For many multisubunit proteins, the folding reaction begins by the transition of unfolded monomers into association-competent monomers. This initial unimolecular reaction is succeeded by one or more association steps and is often terminated by an additional unimolecular rearrangement or "shuffling" of transitory oligomeric intermediates to the final native state. Obviously, such a folding process can be very complex and elementary steps have been characterized in only a few cases [reviews by Goldberg (1985) and Jaenicke (1987)]. For example, folding of the dimeric β_2 subunit of tryptophan synthase has a sequential unimolecular−bimolecular-unimolecular pathway (Zetina & Goldberg, 1980, 1982; Blond & Goldberg, 1985). Dimeric cytoplasmic malate dehydrogenase folds through parallel pathways involving monomeric and dimeric intermediates (Rudolph et al., 1986). Association-competent and non-competent monomers as well as transitory dimers have been described for dimeric luciferase (Ziegler et al., 1993). Folding of the small dimeric trp aporepressor protein is characterized by an extremely rapid interchange between unfolded, partially folded, and completely folded monomers followed by two sequential dimerization steps (Gittelman & Matthews, 1990; Mann & Matthews, 1993). Folding of the dimeric P22 Arc repressor follows a simple two-state mechanism under most conditions (Milla & Sauer, 1994; Waldburger et al., 1996).

Leucine zippers (coiled coils) are perhaps the simplest units that can be classified as small dimeric proteins with a well defined secondary and quaternary structure. Hence leucine zippers should provide good models to study the elementary steps of coupled folding and association processes. Leucine zippers consist of two peptides in an approximately α-helical conformation wound around each other at a 20° angle to form a coiled coil or superhelix. The structure is based on a repeating seven-residue motif, (*a b c d e f g*)$_n$, in which Leu, Val, and Ile are frequently at the *a*

† This work was supported in part by the Swiss National Science Foundation and the Kommission für Wissenschaftliche Forschung.

* Corresponding author.
‡ Biochemisches Institut der Universität Zürich.
§ Present address: Department of Biological Chemistry and Molecular Pharmacology, Harvard Medical School, 240 Longwood Ave, Boston, MA 02115.
|| H.W. and L.L. have contributed equally to this work.
⊥ Present address: Center for Advanced Research in Biotechnology, University of Maryland, 9600 Gudelsky Drive, Rockville MD 20850.
▽ Present address: University of Turku, Department of Biotechnology, Tykistökatu 6 A, FIN-20520 Turku, Finland.
Rheumaklinik, Universitätsspital, Zürich.

⊗ Abstract published in *Advance ACS Abstracts,* December 1, 1996.

S0006-2960(96)01672-8 CCC: $14.00

and *d* positions (Hodges et al., 1972; Landschulz et al., 1988; O'Shea et al., 1989a). Leucine zippers mediate the dimerization of two basic domains to form a DNA-binding site in the basic-leucine-zipper (bZIP) family of transcription factors [reviews by Harrison (1991), Ellenberger (1994), and Hurst (1995)]. Leucine zippers can be homodimers as in the yeast transcription factor GCN4 (Ellenberger et al., 1992; König & Richmond, 1993), or heterodimers as in jun-fos type transcription factors (O'Shea et al., 1989b; Hai & Curran, 1991; Glover & Harrison, 1995).

The earliest study on the kinetics of coiled coil formation was for the very extended coiled coil of tropomyosin, which forms through rapid association of monomeric chains followed by a slow unimolecular reorganization to the final native state (Ozeki et al., 1991). We have used fluorescent derivatives of short model leucine zippers and of GCN4-p1, the 33-residue leucine zipper domain of the yeast transcriptional activator GCN4, to study the kinetics of folding and association by fluorescence stopped-flow experiments. Concentration-dependent and concentration-independent phases were detected for model leucine zippers, indicating monomer/dimer equilibria coupled to equilibria between different conformational isoforms (Wendt et al., 1995). Two unimolecular rearrangement steps subsequent to an association reaction (which could not be seen in the time range of the experiment) were observed for GCN4-p1 (Wendt et al., 1994). Folding was investigated by following relaxation after rapid dilution of a pre-existing monomer/dimer equilibrium and by measuring the rate of strand exchange between different dimers. No denaturant was used in these experiments. In the "classical" approach to the study of protein folding, denaturant unfolded protein is rapidly diluted into benign buffer and refolding is monitored from the change of spectroscopic parameters. Using stopped-flow CD measurements combined with rapid dilution from (and into) denaturant, folding (unfolding) of GCN4-p1 was found to obey a simple two-state reaction with no indication of unimolecular reorganization steps (Zitzewitz et al., 1995). The reason for this discrepancy to our results is not known but could be due either to the nature of the spectroscopic probe, a local fluorescence group (Wendt et al., 1994) *versus* a global spectroscopic parameter (Zitzewitz et al., 1995), or to the different experimental approach, a small and rapid disturbance of the monomer/dimer equilibrium in benign buffer (Wendt et al., 1994) *versus* a rapid dilution from high to low concentrations of urea (Zitzewitz et al., 1995).

Here we report on the folding and association of a heterodimeric leucine zipper composed of an acidic and a basic 30-residue peptide chain. The acidic chain (chain A) had Glu and the basic chain (chain B) had Lys in all the *g* and *e* positions. Each chain alone was essentially unstructured and monomeric because of electrostatic repulsion between like charges. The charges were neutralized in the heterodimer A:B. This feature had been exploited previously by several investigators to design heterodimeric model leucine zippers that were several orders of magnitude more stable than the corresponding homodimers (Graddis et al., 1993; O'Shea et al., 1993; Myszka & Chaiken, 1994; Krylov et al., 1994; Zhou et al., 1994; Kohn et al., 1995).

The kinetics of folding of the heterodimeric model leucine zipper were measured by (i) mixing of the isolated chains in the stopped-flow instrument and (ii) by following the rates of strand exchange between fluorescent and non-fluorescent heterodimers. Fluorescent probes were placed in two different positions: fluorescein was attached to the N-terminus via a triglycine spacer or a single Trp was placed in a central *b* position. Fluorescence emission of the fluorescein group was quenched in the parallel coiled coil, presumably through self-quenching (Wendt et al., 1994). The intrinsic fluorescence of Trp increased on folding.

MATERIALS AND METHODS

Peptide Synthesis and Purification. Peptides were synthesized on a 433A peptide synthesizer (Applied Biosystems), using the Rink amide MBHA resin from Novabiochem, the 9−fluorenylmethyloxycarbonyl (N^{α}-Fmoc) protection strategy, and carboxyl group activation by *O*-benzotriazol-1-yl-*N*,*N*,*N*′,*N*′-tetramethyluroniumhexafluorophosphate/*N*,*N*-diisopropylethylamine. The N-terminal residue was acetylated by reaction of the resin-bound and side chain-protected peptide with a 10-fold molar excess of acetic anhydride and a 5-fold molar excess of diisopropylethylamine (or triethylamine) in dichloromethane (or dimethylformamide). Attachment of N-terminal Flu, separated from the coiled coil sequence by a triglycine spacer, deprotection and cleavage from the resin was performed as described by Wendt et al. (1995). Crude peptides were desalted on a Sephadex-G25 column in 1 M acetic acid. Final purification was achieved by reversed phase high-performance liquid chromatography on a semipreparative C8 column (Machery & Nagel) eluted with binary gradients of acetonitrile/water containing 0.1% or 0.085% trifluoroethanol. Purity of peptides was controlled by amino acid analysis and ion spray mass spectrometry. Peptide concentrations were determined by amino acid analysis on an on-line PTH−amino acid analyzer (Applied Biosystems Inc., model 120A) and by UV absorption in 6 M guanidinium hydrochloride (Edelhoch, 1967). Concentrations are always expressed as total peptide (monomer) concentration, e.g., 1 μM peptide corresponds to 0.5 μM dimeric leucine zipper.

Buffers. All experiments were performed at 25 °C in 10 mM sodium phosphate, pH 7.2, containing 50−500 mM NaCl. Ionic strength values were calculated with the program EQUIL (MicroMath Inc.).

Stopped-Flow Experiments. Measurements were made on an SF-61 stopped-flow spectrofluorimeter (High Tech Scientific Ltd., Salisbury, U.K.). The dead time of the instrument, determined by the dilution of fluorescein into buffer, was approximately 1 ms. Excitation of the fluorescein group was at 492 nm, and emission was measured above 530 nm (cut-off filter OG530). Excitation of the intrinsic Trp fluorescence was at 280 nm and emission was measured above 320 nm (cutoff filter WG320). The instrument time constant was 10 ms for time domains >1 s and 3.3 ms for time domains <1 s. The results of 8−12 syringe firings were averaged for each kinetic trace.

Folding after Rapid Mixing of Monomeric Peptides. Equal volumes of equimolar peptide solutions were mixed and the fluorescence increase (association of A_W with B or of B_W with A) or the fluorescence decrease (association of Flu-A with Flu-B) was monitored (see Results for nomenclature of peptides). Experiments were repeated at 3 to 10 different peptide concentrations in the range 0.25−10 μM. No change of fluorescence was seen on mixing of Flu-A with Flu-A or A_W with A_W. From such control experiments, which set an

upper bound to the fluorescence at time zero, it followed that the measured amplitudes observed on formation of the heterodimers accounted for >95% of the change of fluorescence.

Strand Exchange between Pre-Formed Leucine Zippers. Flu-A:Flu-B in one syringe and non-fluorescent A:B in the other syringe were mixed (equal volumes and equal concentrations), and the fluorescence increase caused by the formation of Flu-A:B and A:Flu-B through strand exchange was monitored (Wendt et al., 1995). Experiments were done at three to six peptide concentrations in the range 0.25−10 μM.

Strand Exchange between Pre-Formed Leucine Zippers and Monomers. Pre-formed leucine zipper A_W:B at a concentration of 0.5, 1, or 2 μM was placed in one syringe, and peptide A at a concentration of 5, 10, or 20 μM in the other syringe. Equal volumes were mixed to achieve strand exchange between the pre-formed leucine zipper and a 10-fold excess of monomeric peptide. The same experiments were repeated with $A:B_W$ and excess of B. The time course of the fluorescence decrease was monitored.

Data Analysis. Using the nonlinear least-squares curve fitter provided by the program Sigma Plot (version 3.10 for Windows), the time course of the fluorescence decrease observed on mixing Flu-A and Flu-B was analyzed initially by eq 1 to test if the reaction had one, two, or more kinetic phases.

$$F(t) = \sum_{i-1}^{n}\left(\frac{\Delta F_{max}(i)\exp[-t/\tau_i]}{1 + q'/\Delta F_{max}(i)(1 - \exp[t/\tau_i])}\right) + F_\infty \quad (1)$$

$F(t)$ is the total amplitude at time t, $\Delta F_{max}(i)$ is the maximum amplitude of phase i, F_∞ is the amplitude at infinite time, and τ_i is the relaxation time of phase i. The term $q'\Delta F_{max}(i)(1 - \exp[t/\tau_i])$ in the denominator corrects for the unfolding/dissociation reaction (Bernasconi, 1976; Gittelman & Matthews, 1990). In the case of the reaction of A_W with B (or A with B_W), the fluorescence increase was transformed to a signal decrease to conform with eq 1. Stopped-flow traces were analyzed as one- and two-phase reactions (n = 1 or 2). The statistical quality of the fits as revealed by the randomness of the residual plots showed that no improvement was achieved by a fit to two phases. Therefore, all further analyses were performed assuming a single phase corresponding to the two-state mechanism

$$M_A + M_B \rightleftharpoons D \quad (2)$$

where M_A and M_B are the acidic and basic monomer, respectively, and D is the heterodimer. In the case of a reaction between equally concentrated monomeric chains ($[M_A] = [M_B]$), a condition that was fulfilled in all of the experiments, the time course of the fluorescence change is described by the equations

$$F(t) = \Delta F_{max}\left(\frac{[M]}{[M_0]}\right) + F_\infty \quad (3)$$

$$F(t) = F_0 + \Delta F_{max}\left(1 - \frac{[M]}{[M_0]}\right) \quad (4)$$

$[M] = [M_A] = [M_B]$ is the concentration of each monomer at time t. $[M_0] = [M_{A0}] = [M_{B0}]$ is the total concentration of each peptide. At time zero, $[M] = [M_0]$. F_0 and F_∞ are the fluorescent signal at time zero and at infinite time, respectively. ΔF_{max} is the maximum change of fluorescence. Equation 3 describes the fluorescence decrease for the reaction of Flu-A with Flu-B. Equation 4 describes the fluorescence increase observed when A_W reacts with B or A with B_W.

If both peptides have the same concentration and if equal volumes of both peptides are mixed in the stopped flow apparatus, the disappearance of the monomeric chains can be described by

$$-\frac{d[M]}{dt} = k_{on}[M]^2 - k_{off}[D] \quad (5)$$

where k_{on} and k_{off} are the rate constant of association and dissociation, respectively. After substitution of [D] by ($[M_0]$ − [M]) and rearranging, the decrease of [M] can be described by

$$-\frac{d[M]}{dt} = k_{on}[M_0]\left(\frac{[M]^2}{[M_0]} + \frac{k_{off}[M]}{k_{on}[M_0]} - \frac{k_{off}}{k_{on}}\right) \quad (6)$$

and, after integration,

$$[M] = \left[\frac{zb + zs - b + s}{1 - z}\right]\frac{[M_0]}{2} \quad (7)$$

where

$$b = \frac{k_{off}}{k_{on}[M_0]}$$

$$s = \sqrt{4b + b^2}$$

$$z = \left(\frac{2 + b - s}{2 + b + s}\right)\exp(-sk_{on}[M_0]t)$$

Equations 3 and 4 in which [M] was substituted by eq 7 were fitted to the fluorescence signal observed after mixing the monomeric chains (Figure 2). In principle, the fits should provide values for k_{on}, k_{off}, ΔF_{max}, and F_0 or F_∞. However, as already noted by Milla and Sauer (1994) who used an analogous equation to analyze the folding of the homodimeric Arc repressor P22, simultaneous determination of the four parameters tended to produce poor estimates of k_{on} and k_{off} because of ill-defined arrays during the fitting procedure. The problem could be overcome by fixing ΔF_{max} or F_0 or F_∞ during fitting. The fixed values were taken from an initial fit that gave poorer values for k_{on} and k_{off}. Alternatively, good fits were obtained when $K_a = k_{on}/k_{off}$ was known from an independent experiment (see below) so that k_{on}/k_{off} could be fixed during the initial fitting. The two procedures yielded equivalent results.

The concentration-independent rate constant for strand exchange, k_{ex}, was obtained from the fit of a single exponential reaction to the stopped-flow trace (Wendt et al., 1995).

Association Constants from Equilibrium Fluorescence Measurements. Measurements were made on a SPEX Fluorolog spectrofluorimeter or a Perkin Elmer LS-5 luminescence spectrometer at 25 °C and using cuvettes of 1 cm pathlength. Spectra were measured in 1 nm steps with 1 or

2 s integration time. Trp emission was monitored between 340 and 380 nm (excitation 295 nm). Fluorescein emission was monitored from 500 to 600 nm (excitation 492 nm).

To measure K_a of the dimer Flu-A:Flu-B, fluorescence spectra of Flu-A, Flu-B, and of a 1:1 mixture of Flu-A and Flu-B were measured in the range 50 nM to 1.2 μM peptide concentration. Aliquots of the peptides (0.5−20 μL from 22.5 μM stock solutions) were added to 2.5 mL of buffer, and the fluorescence spectrum was recorded after each addition. At each concentration $[M_0]$, the fluorescence signal at maximum emission (525 nm) was corrected for dilution and normalized to the total peptide concentration according to

$$F_{\text{norm}} = \frac{F_{\text{Flu-A}} + F_{\text{Flu-B}} - F_{\text{Flu-A+Flu-B}}}{[M_0]} \quad (8)$$

$F_{\text{Flu-A}}$, $F_{\text{Flu-B}}$, and $F_{\text{Flu-A+Flu-B}}$ are the observed fluorescence emission of the single chains and the 1:1 mixture of the two chains, respectively. K_a was obtained from nonlinear least-squares fitting to

$$F_{\text{norm}} = F_{\text{norm,max}} \times \{[1 + 2K_a[M_0] - \sqrt{(1 + 2K_a[M_0])^2 - 4K_a^2[M_0]^2}]/2K_a[M_0]\} \quad (9)$$

with K_a and $F_{\text{norm,max}}$ as the fitting parameters. $F_{\text{norm,max}}$ is the maximum fluorescence emission at saturation (infinite concentration). The second term on the right of eq 9 equals $[D]/[M_0]$, which is the fraction of each peptide in the coiled coil conformation. Note that eq 9 is valid only for 1:1 mixtures of peptide chains.

K_a for dimers A_W:B and A:B_W was determined by titration of 2 mL of 0.5 or 1 μM A_W (or B_W) with increasing amounts of B (or A) added in small aliquots from an appropriately concentrated stock solution. Fluorescence emission was measured after each addition and plotted against the total concentration of the added non-fluorescent peptide. Data were analyzed by

$$\Delta F = \Delta F_{\text{max}} \times \{[1 + K_a([M_{A0}] + [M_{B0}]) - \sqrt{(1 + K_a([M_{A0}] + [M_{B0}]))^2 - 4K_a^2[M_{A0}][M_{B0}]}]/2K_A[M_{F0}]\} \quad (10)$$

ΔF is the observed change of fluorescence and ΔF_{max} is the maximum fluorescence change at saturation. $[M_{A0}]$ and $[M_{B0}]$ are the total concentration of the acidic and basic peptide, respectively. $[M_{F0}]$ is the total concentration of the peptide that contained the fluorescent Trp residue, that is, $[M_{F0}]$ was equivalent to either $[M_{A0}]$ or $[M_{B0}]$. The second term on the right of eq 10 is $[D]/[M_{F0}]$, which is the fraction of fluorescent peptide in the leucine zipper.

Debye−Hückel Analysis. The mean rational activity coefficient, *f*, relates to the activity of a solution expressed in dimensionless mole fractions. The electrostatic component of *f* for a 1:1 electrolyte like NaCl is defined by

$$\log f_{\pm}^{\text{el}} = -\frac{A|Z_1Z_2|\sqrt{\mu}}{1 + Ba\sqrt{\mu}} \quad (11)$$

Up to about 0.5 M ionic strength, $f_{\pm}^{\text{el}}$ is the major contributor to the rational activity coefficient (Robinson & Stokes, 1959). Z_1 and Z_2 are the charges of the electrolyte, *a* is the distance of closest approach of the ions, and *A* and *B* are constants involving the absolute temperature and the dielectric constant (Robinson & Stokes, 1959; Debye & Hückel, 1923). Values of *A* and *B* for 25 °C and water were taken from Appendix 7.1 of Robinson and Stokes (1959). For NaCl, a value of $a = 4.62$ Å was used, which corresponds to the sum of the radii of Na^+ and Cl^- including the immobilized electrostricted first hydration layer (Marcus, 1994). The small amount of phosphate present in the buffer was neglected in the calculation.

RESULTS

Structure of the Heterodimeric Leucine Zipper. The sequence of the acidic peptide was X_1-EYQA**L**E**K**E**V**AQ-**L**E**A**E**N**X_2A**L**E**K**E**V**AQ**L**E**H**EG-amide and that of the basic peptide X_1-EYQA**L**K**K**K**V**AQ**L**K**A**K**N**X_2A**L**K**K**K**V**AQ**L**-K**H**KG-amide (residues at *a* and *d* positions are in bold, and those at *e* and *g* positions are underlined). The following abbreviations were used to designate the different fluorescent and non-fluorescent peptides. A, B: non-fluorescent, N^{α}-acetylated peptides (X_1 = acetyl, X_2 = Q). Flu-A, Flu-B: peptides with a fluorescein group attached to the N-terminus via a triglycine spacer (X_1 = 5-carboxyfluoresceinyl-Gly-Gly-Gly, X_2 = Q). A_W and B_W: fluorescent peptides containing a Trp residue in *b* position 17 (X_1 = acetyl, X_2 = W). Heterodimers were abbreviated as A:B, Flu-A:Flu-B, A_W:B, and A:B_W. At neutral pH, A and A_W had a calculated net charge of −7, and B and B_W of +9. The calculated net charges of Flu-A and Flu-B were −8 and +8, respectively.

The pattern of hydrophobic residues in the *a* and *d* positions was that of the leucine zipper domain of the transcription factor GCN4, except for the first *a* position which was Tyr and served as a chromophore to determine peptide concentration. The pattern L^d V^a L^d N^a L^d V^a L^d (superscripts indicate position in heptad) stabilizes a parallel and in-register orientation of the dimer (Ellenberger et al., 1992; Lumb & Kim, 1995a; Junius et al., 1995). Helix-stabilizing residues were chosen for positions *b*, *c*, and *f* located on the solvent-exposed surface of the coiled coil.

Previous sedimentation equilibrium analysis of equimolar amounts of peptide A and B (total chain concentration 100−300 μM) revealed a homogeneous population of molecules sedimenting with an apparent molecular mass of 6710 ± 85 Da, close to the calculated dimer mass of 6921 Da. Peptides A and B alone sedimented with the mass of the monomer (Thomas et al., 1995). These experiments confirmed that the heterodimer A:B was the only significantly populated species at micromolar peptide concentrations. To test if the hydrophobic core of the coiled coil structure was tight and well packed, binding of the fluorescent dye ANS[1] was tested. This dye binds to hydrophobic patches and to clusters of loosely packed hydrophobic residues (Semisotnov et al., 1991). The increase in fluorescence on addition of excess ANS was less than 5% of the total fluorescence signal (not shown). The inability to bind ANS indicated that the heterodimeric leucine zipper had a compact, native-like

[1] Abbreviations: μ, ionic strength; ANS, 8-anilino-2-naphthalenesulfonic acid.

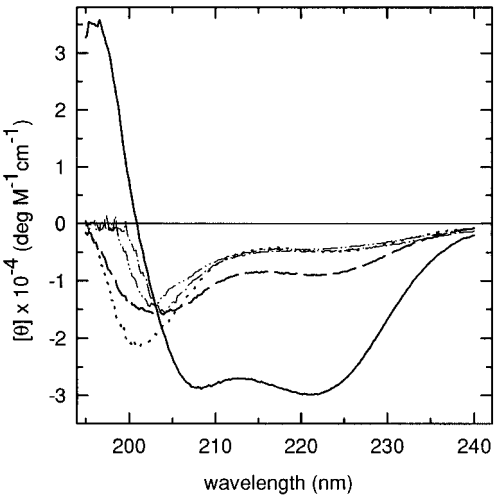

FIGURE 1: CD spectra of peptide A (•••), peptide B (- - -) and equimolar amounts of peptide A and B (—) measured at 7 °C. For comparison, the spectra of peptide A (- • -) and peptide B (- •• -) measured under unfolding conditions at 75 °C are also shown. Total peptide concentration was 0.1 mM in 10 mM sodium phosphate, 75 mM NaCl, pH 7.2.

structure and could be regarded as a native "mini protein" (Betz et al., 1995).

The parallel orientation of the two strands of A:B was confirmed by the observation of an 8-fold lower fluorescence emission in Flu-A:Flu-B as compared to Flu-A:B and A:Flu-B (data not shown and Wendt et al., 1995). Insignificant quenching was expected in the case of the antiparallel arrangement in which the fluorophores are about 50 Å apart.

The CD spectrum of equimolar mixtures of peptides A and B exhibited the characteristic spectral signature of the α-helical conformation (Figure 1). The ratio of the two minima centered at 221 nm and 208 nm was 1.04 for the heterodimer A:B. This value is thought to be typical for interacting parallel α-helices (Zhou et al., 1992). CD-spectra of peptides A and B in isolation when measured at μ below about 0.8 M indicated non-helical, quasi random coil conformations (Figure 1). The spectra of peptide A were very similar when measured at 7 and 75 °C, demonstrating a random coil nature of peptide A under the temperature conditions of the kinetic experiments. At low temperature, peptide B showed a very weak signal in the α-helix region, which, however, disappeared above 30 °C [Figure 1 and Jelesarov and Bosshard (1996)]. Thus, peptide B seems to have retained some structure at temperatures below 30 °C. At high ionic strength, both chains in isolation exhibited typical helix spectra. The ellipticity at 222 nm of chain B corresponded to near 100% helix content in 2 M NaCl and that of chain A in 3.7 M NaCl (not shown). Because of the amphipathic nature of the peptide chains, a helical monomeric peptide conformation is implausible and, therefore, the development of helix at high μ indicated the formation of homomeric coiled coils.

Fluorescent Stopped-Flow Experiments. Figure 2 shows representative examples of stopped-flow traces observed after rapid mixing of acidic and basic peptides. In the reaction of the fluorescein-labeled peptides, the fluorescence decrease was large and the signal-to-noise ratio was very high (Figure 2A). The increase of the intrinsic Trp fluorescence in A_W:B or A:B_W was smaller, and the signal-to-noise ratio was lower

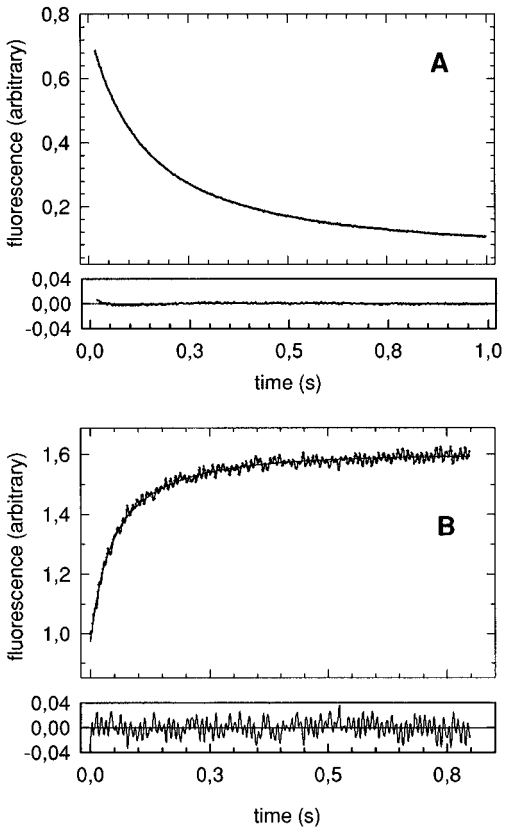

FIGURE 2: Example of fluorescence stopped-flow experiments. (A) Reaction of equal volumes of 0.9 μM Flu-A and Flu-B, $\mu = 0.275$ M. The solid line is a best fit according to eq 3 with $k_{on} = 8.36 \times 10^6$ M^{-1} s^{-1}, $k_{off} = 0.052$ s^{-1}, $\Delta F_{max} = 0.782$, and $F_\infty = 0$. (B) Reaction of equal volumes of 1.8 μM A and B_W, $\mu = 0.205$ M. The solid line is a best fit according to eq 4 with $k_{on} = 1.01 \times 10^7$ M^{-1} s^{-1}, $k_{off} = 0.208$ s^{-1}, $\Delta F_{max} = 0.695$, and $F_0 = 0.952$. The residuals of the fits are shown below panel A and B, respectively. Note the difference in the quality of the fluorescence signal in panel A (fluorescein, excitation 492 nm, emission >530 nm) and panel B (Trp, excitation 280 nm, emission >320 nm).

(Figure 2B). The fluorescence traces could be described by a two-state reaction involving only the unfolded chains and the folded heterodimer. Because the measured amplitudes accounted for more than 95% of the overall change in fluorescence, any change of fluorescence during the dead time of mixing must have been very small. Hence, there was no evidence for the accumulation of intermediates within <1 ms.

To simplify data analysis, all experiments were conducted by mixing equal volumes of equally concentrated solutions of peptides. Under these conditions, the fluorescence decrease (formation of Flu-A:Flu-B) and the fluorescence increase (formation of A_W:B and A:B_W) is described by eqs 3 and 4, respectively. k_{on} and k_{off} were obtained by nonlinear least-squares fitting with the help of eq 7, which describes the decrease of the monomer concentration with time. Values of k_{on} and k_{off} measured at different ionic strengths are shown in Tables 1 and 2. On-rate constants were essentially the same for the formation of Flu-A:Flu-B, A_W:B, and A:B_W, respectively. The rates increased significantly when the ionic strength was lowered, indicating an electrostatic contribution to the association reaction. The rates of dissociation depended only weakly on ionic strength and were 3−5 times higher for A_W:B and A:B_W than for Flu-A:Flu-B.

Table 1: Kinetic Constants for the Two-State Folding and Association of the Heterodimeric Leucine Zipper Flu-A:Flu-B[a]

ionic strength (M)	$k_{on} \times 10^{-6}$ [b] (M^{-1} s^{-1})	$k_{off} \times 10^{2}$ [b] (s^{-1})	$k_{ex} \times 10^{2}$ [c] (s^{-1})	$(K_a = k_{on}/k_{off}) \times 10^{-7}$ (M^{-1})	$K_a \times 10^{-7}$ [d] (M^{-1})
0.074	72.2 ± 12.3 (7)	3.8 ± 0.5 (7)	3.2	190 ± 41	65 ± 7
0.103	33.3 ± 3.7 (4)	3.8 ± 0.2 (4)	3.7 ± 0.3 (4)	87.6 ±10.8	nd
0.144	22.5 ± 3.0 (4)	5.2 ± 0.4 (4)	4.9 ± 0.3 (4)	43.3 ± 6.7	47.7 ± 4.7
0.175	14.9 ± 1.5 (10)	5.3 ± 0.4 (10)	5.2 ± 0.4 (4)	28.1 ± 3.5	nd
0.205	nd	nd	nd	−	23.3 ± 4.0
0.275	8.40 ± 0.70 (4)	5.1 ± 0.5 (4)	4.9	16.5 ± 2.1	15.0 ± 2.0
0.525	3.69 ± 0.26 (5)	10.1 ± 2.5 (5)	8.5	3.65 ± 0.94	4.6 ± 0.5

[a] Errors are SEM of *n* independent measurements performed at total peptide concentrations in the range 0.25−10 μM; *n* is given in parentheses. [b] From fit of fluorescence decrease (Figure 2A) with eqs 3 and 7. [c] Rate constant of strand exchange between Flu-A:Flu-B and A:B. [d] From equilibrium measurements (Figure 3A) and data analysis according to eq 9. Errors are standard errors of the fitting procedure.

Table 2: Kinetic Constants for the Two-State Folding and Association of the Heterodimeric Leucine Zippers A_W:B and A:B_W[a]

ionic strength (M)	$k_{on} \times 10^{-6}$ [b] (M^{-1} s^{-1})	k_{off} [b] (s^{-1})	k_{ex} [c] (s^{-1})	$(K_a = k_{on}/k_{off}) \times 10^{-7}$ (M^{-1})	$K_a \times 10^{-7}$ [h] (M^{-1})
0.074	32.2 ± 2.6 (8)[d]	0.184 ± 0.008 (8)[d]	0.119 ± 0.004 (4) [f]	17.5 ± 1.6	15 ± 8 [i]
0.074	38.9 ± 0.73 (6)[e]	0.164 ± 0.028 (6)[e]	0.110 ± 0.005 (4) [g]	23.7 ± 4.1	19 ± 9 [k]
0.144	25.7 ± 1.7 (6)[d]	0.217 ± 0.018 (6)[d]	0.179 ± 0.009 (4) [f]	11.8 ± 1.2	nd
0.144	22.9 ± 3.9 (8)[e]	0.205 ± 0.006 (8)[e]	0.180 ± 0.012 (4) [g]	11.2 ± 1.9	nd
0.205	12.1 ± 2.0 (4)[d]	0.228 ± 0.003 (4)[d]	0.222 ± 0.015 (4) [f]	5.31 ± 0.88	4.6 ± 1.2 [i]
0.205	10.3 ± 0.6 (4)[e]	0.205 ± 0.005 (4)[e]	0.201 ± 0.012 (4) [g]	5.02 ± 0.32	nd
0.275	5.29 ± 1.81 (4)[d, l]	0.238 ± 0.014 (4)[d]	nd	2.22 ± 0.77	1.9 ± 0.6 [i]
0.325	6.53 ± 0.98 (4)[d]	0.240 ± 0.020 (4)[d]	0.269 ± 0.005 (4) [f]	2.72 ± 0.47	1.6 ± 0.5 [i]
0.325	4.79 ± 0.57 (4)[e]	0.251 ± 0.009 (4)[e]	0.248 ± 0.013 (4) [g]	1.91 ± 0.24	1.4 ± 0.5 [k]

[a] Errors are SEM of *n* independent measurements performed at total peptide concentrations in the range 0.25−10 μM; *n* is given in parentheses. [b] From fit of fluorescence increase (Figure 2B) with eqs 4 and 7. [c] Rate constant of strand exchange. [d] Reaction of A_W with B. [e] Reaction of A with B_W. [f] Strand exchange between A_W:B and excess of A. [g] Strand exchange between A:B_W and excess of B. [h] From equilibrium measurement (Figure 3B) and data analysis according to eq 10. Errors are standard errors of the fitting procedure. [i] From titration of A_W with B. [k] From titration of B_W with A. [l] $k_{on} = (4.66 \pm 0.85) \times 10^6$ M^{-1} s^{-1} from experiment conducted under pseudo-first-order conditions, see text for details.

As a control, the reaction of A_W with B at $\mu = 275$ mM was measured in an experiment conducted under pseudo-first-order conditions with 0.8 μM A_W in one syringe and 8, 17, 26, or 34 μM B in the other syringe. A plot of k_{app} (apparent rate constant) against the total concentration of B was linear. k_{on} calculated from the slope of this plot was $(4.66 \pm 0.85) \times 10^6$ M^{-1} s^{-1}, in very good agreement with $k_{on} = (5.29 \pm 1.81) \times 10^6$ M^{-1} s^{-1} obtained from mixing equal amounts of A_W and B and data analysis by eq 7 (Table 2). k_{off} was too small to be accurately determined from the *y*-intercept of the linear plot of k_{app} against [B] (not shown).

The rates of strand exchange were measured by mixing fluorescent with non-fluorescent peptides. These rates did not depend on concentration, demonstrating that the dissociation of the dimer into monomers was the rate-limiting step of strand exchange (Wendt et al., 1995). Strand exchange exhibited a single exponential phase, and, within the limit of errors, k_{ex} from strand exchange was equivalent to k_{off}. This gives further credence to the validity of a two-state mechanism for which $k_{off} = k_{ex}$ [see Appendix A in Wendt et al. (1995)]. The off-rate constants were slightly lower at low ionic strength.

Determination of Equilibrium Association Constants. K_a was determined under equilibrium conditions by measuring the change of the fluorescence signal with peptide concentration. For Flu-A:Flu-B, the fluorescence emission of 1:1 mixtures of the two peptides when normalized to the total peptide concentration showed a typical saturation curve from which K_a could be calculated (Figure 3A and eq 9). Similarly, K_a of A_W:B or A:B_W was obtained by fluorescence titration experiments (Figure 3B and eq 10). K_a calculated as k_{on}/k_{off} was in good agreement with K_a determined directly under equilibrium conditions, again in concordance with a two-state folding mechanism. A_W:B and A:B_W were somewhat less stable than Flu-A:Flu-B. The difference in stability was caused by the 3−5 times higher k_{off} for the Trp-containing zippers.

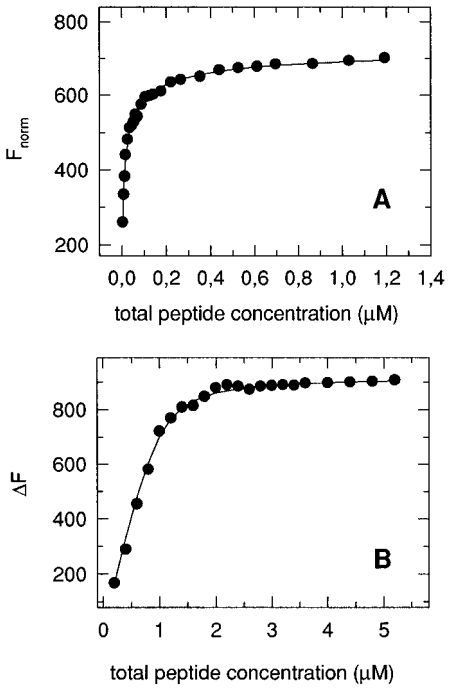

FIGURE 3: Examples of equilibrium fluorescence titration experiments to determine K_a. (A) Normalized fluorescence signal (eq 8) observed for 1:1 mixtures of Flu-A and Flu-B in the range 4.4×10^{-9} to 1.4×10^{-6} M total peptide concentration and $\mu = 0.275$ M. The solid line is a best fit according to eq 9 with $K_a = 1.73 \times 10^8$ M^{-1} and $F_{norm,\,max} = 745$. (B) Change of fluorescence observed on titration of 1 μM A_W with 0.2 to 5.2 μM B. The solid line is a best fit according to eq 10 with $K_a = 1.4 \times 10^7$ M^{-1} and $\Delta F_{max} = 920$.

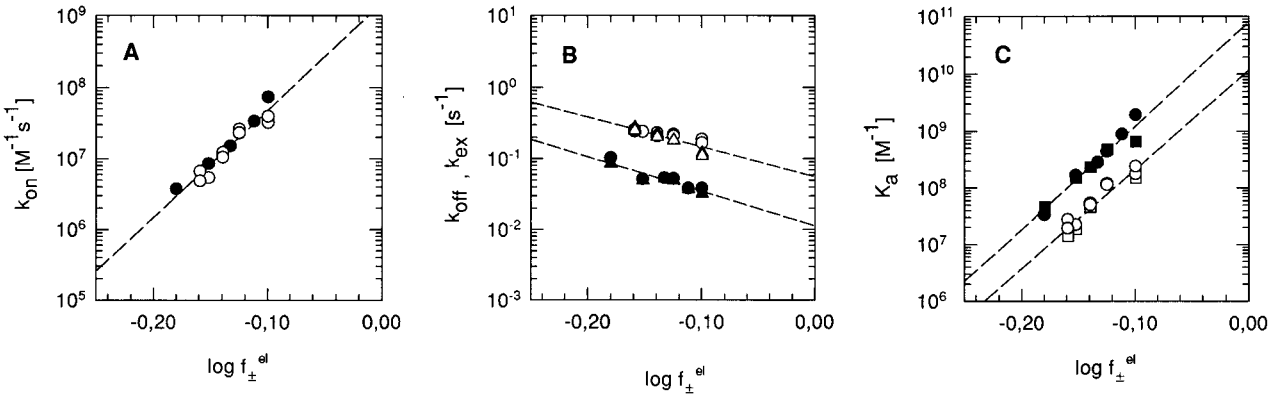

FIGURE 4: Dependence of rate constants and equilibrium association constants on ionic strength. The rate and equilibrium constants of Tables 1 and 2 are plotted on a logarithmic scale against the electrostatic component of the mean rational activity coefficient for NaCl, $f_{\pm}^{el}$ (eq 11). A linear correlation is expected if the association reaction is dominated by electrostatics (Schreiber & Fersht, 1996). Filled symbols refer to Flu-A:Flu-B. Open symbols refer to A_W:B and A:B_W. (A) k_{on} for the reaction of Flu-A with Flu-B (●), A_W with B and A with B_W (○). (B) k_{off} (●, ○) and k_{ex} (▲, △). (C) K_a calculated from k_{on}/k_{off} (●, ○) and determined directly under equilibrium conditions (■, □). The dashed lines are best fits according to eq 12.

Analysis of the Electrostatic Effect. The dependence on ionic strength of the association of oppositely charged proteins can be described by an extended Debye−Hückel theory developed by Koppenol (1980). The theory describes the relationship of size, net charge and molecular dipole moment of the interacting molecules to the rate and equilibrium constants. According to this theory, a Debye−Hückel plot of log k_{on} *versus* $(\mu)^{1/2}$ shows an upward concave shape the curvature of which strongly depends on the molecular dipole moment of the associating proteins, that is, on the surface distribution of charges (Koppenol, 1980). Indeed, a plot of log k_{on} *versus* $(\mu)^{1/2}$ exhibited a concave upward curvature (not shown). However, the limiting k_{on} at zero ionic strength could not be extrapolated from the curve because the molecular dipole moments of the associating unfolded peptide chains are not defined. As an alternative, we chose the simpler yet less rigorous analysis of Figure 4 to quantify the ionic strength dependence of the rate and equilibrium constants. In Figure 4, log k_{on}, log k_{off}, and log K_a are plotted against the electrostatic component of the mean rational activity coefficient for NaCl, $f_{\pm}^{el}$ (eq 11). It has been pointed out that a plot of log k_{on} *versus* log $f_{\pm}^{el}$ is linear if the rate-limiting step of association is governed mainly by the electrostatic potential between the associating molecules (Schreiber & Fersht, 1996). The reason is that the electrostatic potential is proportional to $RT \ln f_{\pm}^{el}$ (Robinson & Stokes, 1959) and that the activation free energy of the association reaction is proportional to $RT \ln k_{on}$. By the same argument, log k_{off} and log K_a should linearly depend on log $f_{\pm}^{el}$. Indeed, a linear correlation between the rate and equilibrium constants of Tables 1 and 2 and log $f_{\pm}^{el}$ was obtained. The dashed lines in Figure 4 fit the equation

$$\log k = \log k(0) + m \log f_{\pm}^{el} \qquad (12)$$

where k is k_{on}, k_{off}, or K_a, and $k(0)$ is the corresponding value at zero ionic strength, and m is the slope. The extrapolated $k_{on}(0) = 9.2 \times 10^9$ M^{-1} s^{-1} (Figure 4A) approaches the range of the diffusion limit of association of a coiled coil. This limit was estimated at $4 \times 10^8 - 4 \times 10^9$ M^{-1} s^{-1} for an extended homomeric coiled coil (Ozeki et al., 1991) but could be higher for the association of shorter and oppositely charged peptide chains (Eigen & Hammes, 1963).

In Figure 4B, the limiting values are $k_{off}(0) = 0.01$ s^{-1} for Flu-A:Flu-B, and 0.06 s^{-1} for A_W:B and A:B_W. The limiting equilibrium association constants are $K_a(0) = 8 \times 10^{10}$ M^{-1} for Flu-A:Flu-B, and 1×10^{10} M^{-1} for A_W:B and A:B_W (Figure 4C). It should be noted that this linear extrapolation to zero ionic strength has no solid physical basis as it does not take into consideration the size and charge distribution on A, B, and A:B (Koppenol, 1980). The extrapolated values have to be regarded as rough approximations.

At high ionic strength, the charges on the associating peptide chains are screened and the association is no longer dominated by electrostatics. Indeed, the CD spectra of the single chains measured at high ionic strength indicated the formation of homomeric coiled coils despite the many opposing charges in A:A and B:B or in multiple-chain coiled coils. At $\mu \geq 2$ M both chains showed very considerable helix content and the electrostatic contribution to k_{on} was negligible. According to Figure 4A, k_{on} is 5×10^5 M^{-1} s^{-1} at $\mu = 2$ M (log $f_{\pm}^{el} = -0.23$). This value of k_{on} is very similar to that reported for the homomeric GCN4-p1 leucine zipper peptide (Zitzewitz et al., 1995), the stability of which has no, or only a very small, electrostatic component (Lumb & Kim, 1996). Thus, electrostatic attraction seems to increase k_{on} by 10^3-10^4-fold.

DISCUSSION

Interpretation of Two-State Association/Folding Mechanism. The coupled association and folding reaction can be modeled by a two-state transition between unfolded monomers and folded heterodimers. A two-state mechanism is supported by the following observations: (i) the time course of the reaction shows a single phase irrespective of the location of the fluorescent probe; (ii) the single phase accounts for the entire change of fluorescence in both strand association and strand exchange; (iii) k_{off} obtained from the rapid mixing of monomers and k_{ex} obtained from strand exchange are the same within the limit of errors; (iv) K_a determined directly under equilibrium conditions is the same within error as that calculated from the kinetic constants. Furthermore, isothermal titration calorimetry and thermal unfolding experiments showed that the dependence on temperature of ΔG_{unfold} can be described by a two-state

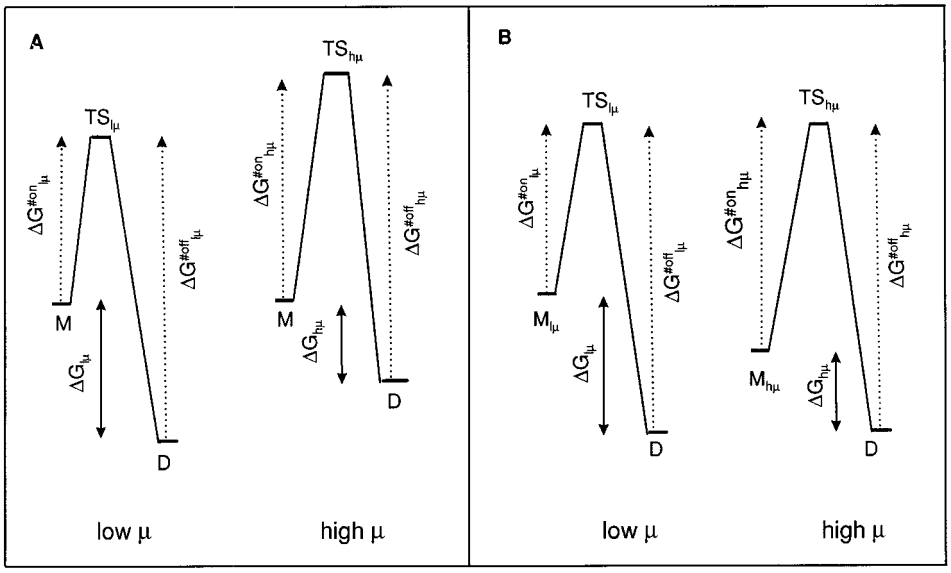

FIGURE 5: Free energy diagram illustrating a hypothetical ionic strength effect on the rate of folding by a change in the stability of the transition state (panel A) or by a change in the stability of the unfolded monomers (panel B). (A) Ionic strength affects the magnitude of the free energy of activation of the forward reaction. Because $\Delta G^{\ddagger}{}_{\mathrm{on}}{}_{l\mu} < \Delta G^{\ddagger}{}_{\mathrm{on}}{}_{h\mu}$, the energies of the transition states differ: $TS_{l\mu} < TS_{h\mu}$. (B) Ionic strength alters the free energy of the unfolded state. At low μ, monomers are more extended and have a higher energy than at high μ where they are thought to be partially collapsed ($M_{l\mu} < M_{h\mu}$). This leads to $\Delta G^{\ddagger}{}_{\mathrm{on}}{}_{l\mu} < \Delta G^{\ddagger}{}_{\mathrm{on}}{}_{h\mu}$. The free energy of the final dimer and of the transition state, respectively, are equal at low and high μ. Both mechanisms (panel A and B) may contribute to the observed ionic strength effect on k_{on} but not k_{off} (see text for further details).

transition between monomeric chains and the A:B heterodimer (Jelesarov & Bosshard, 1996).

Is such a simple mechanism compatible with the formation of an ordered coiled coil from two peptide chains that lack regular structure in the monomeric state? It is important to emphasize that a two-state transition from monomer to dimer must not be interpreted as an all-or-none mechanism comprising only a disordered monomer and a fully native heterodimer (Qian, 1994). Rather, a two-state mechanism means that all molecular conformations can be divided into two groups separated by a high-energy barrier, chiefly disordered monomeric chains, and chiefly ordered heterodimers. Fluctuations of conformation within each group are small compared with the mean structural and energetic difference between the two groups (Qian, 1994). Lack of an observable intermediate, or intermediates, could indicate either that no intermediate was sufficiently populated to lead to a separate kinetic phase or that the intermediate was too short-lived to be seen.

A folding mechanism has to explain the following three premises. First, at a rate of folding close to the diffusion limit almost every collision is successful. Therefore, the highest energy barrier has to be overcome in the formation of the initial collisional complex and subsequent folding to D is along a "down-hill" free energy landscape. Second, helix formation *per se* cannot be rate-limiting since $t_{1/2}$ of the folding reaction is in the range of milliseconds. Folding of an α-helix occurs with a time constant of 10^{-7} s or less (Schwarz, 1965; Hammes & Roberts, 1969) and is thought to be some 3 orders of magnitude faster than the time necessary for intramolecular contact formation (Williams et al., 1996). Third, once the stable heterodimer D is formed, ionic strength has little effect on the back-dissociation into monomers because k_{off} is affected minimally by the salt concentration.

We postulate that the ionic strength changed the height of the initial energy barrier as indicated in Figure 5A. The observed difference in free energy of A:B at low and high μ ($\Delta G_{l\,\mu} > \Delta G_{h\,\mu}$) is accounted for by the difference in the free energies of activation of the forward reaction ($\Delta G^{\ddagger}{}_{\mathrm{on}}{}_{l\mu} < \Delta G^{\ddagger}{}_{\mathrm{on}}{}_{h\mu}$). The activation free energies of the unfolding reaction are nearly equal at low and high μ ($\Delta G^{\ddagger}{}_{\mathrm{off}}{}_{l\mu} \approx \Delta G^{\ddagger}{}_{\mathrm{off}}{}_{h\mu}$). How can low ionic strength lower the activation free energy of folding but not unfolding? One possibility is by steering the oppositely charged monomers into the collisional complex and by electrostatic stabilization of the collisional complex. Large rate increases through electrostatic steering and attraction have been seen in the association of electron transfer proteins (Koppenol & Margoliash, 1982; Margoliash & Bosshard, 1983). A nearly diffusion-limited rate of association is difficult to explain. Since the monomeric chains lack regular structure, one would expect that the initial complex, whose formation is the rate-limiting step at the diffusion limit, has a loose and poorly ordered structure. Long-range and middle-range electrostatic forces may contribute significantly to the stabilization of this initial dimeric state without the need of formation of native-like structure. If so, the rate-limiting transition state might be closer to the unfolded than to the folded state. This idea is supported by very recent work on the coupled association/folding of the P22 Arc repressor, a 53-residue homodimer (Milla & Sauer, 1994; Milla et al., 1995; Waldburger et al., 1996). Mutation of buried polar interactions to buried hydrophobic interactions in the P22 Arc mutant MYL increased the folding rate to near diffusion-limited and shifted the transition state further away from the native state (Waldburger et al., 1996). It is postulated that the folding of a newly introduced hydrophobic cluster in mutant MYL is much faster than the formation of geometrically more demanding ionic interactions in wild type Arc P22. Alanine-substitution mutations suggest that during folding most native interactions take place without the need for proper orientation of the peptide chain in the transition state (Milla et al., 1995). In the present case, the extremely rapid formation of the

extended hydrophobic core of the A:B zipper could be initiated by the formation of a transition state that has relatively little native-like structure. In accord with this postulate and with the premise that helix formation is not rate-limiting is very recent work on the folding of the 33-residue leucine zipper GCN4-p1′ (Sosnick et al., 1996a). There is no widespread formation of helix seen at the the rate-limiting step of folding of this homodimeric zipper structure. The view of a poorly structured transition state stabilized by both electrostatic attraction and yet ill-defined hydrophobic interactions fits into the framework of a nucleation−condensation pathway (Fersht, 1995) or a molecular collapse model (Dill, 1985; Sosnick et al., 1996b). Both of these models explain folding without the formation of stable intermediates and without accretion of stable elements of structure as a prerequisite for successful folding.

A very different phenomenon may add to the strong ionic strength effect on k_{on} but not k_{off}, namely, a change of the free energy of the unfolded monomers with μ (Figure 5B). At low salt, monomers may adopt a more extended conformation because of intramolecular charge repulsion. At high salt, repulsion is weaker and partial collaps of monomers may be facilitated through the many hydrophobic residues in *a* and *d* positions. It is reasonable to assume that the free energy in aqueous buffer of a partially collapsed structure is lower because of the hydrophobic effect. Assuming the highest barrier of the folding pathway is essentially the same at low and high μ, the activation energy to reach this highest barrier will be higher if the single chains are in a partially collapsed state. This is to say that the larger free energy difference of the folding reaction at low μ is caused by a less stable monomeric structure rather than by a lower free energy barrier, the free energy of the final folded dimer being the same at low and high μ (Figure 5B). The influence of the ionic strength on the nature of the unfolded state of chains A and B is currently under investigation in our laboratory and preliminary experiments indicate a small change of the far-UV CD spectrum of chain B, both with temperature and with ionic strength in the range 50−500 mM NaCl (not shown). Nevertheless, we think that an ionic strength effect on the stability of the transition state(s), as illustrated by Figure 5A, contributes more to the increased rate of folding at low ionic strength.

Electrostatic Stabilization of Leucine Zippers. The contribution of salt bridges to the stability and specificity of assembly of coiled coils is under dispute (Lavigne et al., 1996; Lumb & Kim, 1996). Whereas electrostatic repulsion clearly destabilizes the coiled coil conformation (Kohn et al., 1995, and references therein), evidence for stabilizing salt bridges remains elusive. The most direct test for a stabilizing salt bridge is a comparison of pK_a values in the monomeric peptide and in the coiled coil. pK_a values deduced by NMR do not support the existence of salt bridges in a GCN4-type model leucine zipper (Lumb & Kim, 1995b, 1996). Do salt bridges contribute to the stability of the folded A:B dimer? A definite answer cannot be given but the small ionic strength effect on k_{off} seems to indicate that there is no need to postulate specific salt bridges to explain electrostatic stabilization. Assuming the overall fold of the A:B dimer is the same as that of other parallel and dimeric leucine zippers of known X-ray structure (O'Shea et al., 1991; Ellenberger et al., 1992; König & Richmond, 1993; Glover & Harrison, 1995), interchain ionic bonds could be formed between residues at *g* (*g*′) and *e*′ (*e*) positions of the two parallel chains. These salt bridges would be easily screened by salt ions. Therefore, one would expect k_{off} to depend on μ more strongly than was observed if such salt bridges were to contribute significantly to the stability of the folded heterodimer. By this argument one can conclude that interchain ionic bonds confer little extra stability to the folded dimer, which is stabilized predominantly by the hydrophobic effect. A thermodynamic cycle analysis on an extensive series of leucine zipper mutants has provided a value of −0.14 kcal/mol of interchain coupling energy for the pair Glu/Lys located in positions *g*/*e*′ (Krylov et al., 1994). However, this small coupling energy is difficult to interpret and cannot be ascribed to a charge−charge effect alone since the reference side chain in the thermodynamic cycle was the methyl group of Ala.

Electrostatic stabilization without evidence for intermolecular salt bridges was demonstrated for electron transfer complexes whose association is governed by electrostatics (Margoliash & Bosshard, 1983) and can be described by an extended Debye−Hückel theory (Koppenol & Margoliash, 1982). The crystal structure of one such complex between cytochrome *c* and cytochrome *c* peroxidase shows excellent geometrical complementarity between surfaces of opposite potential yet no *bona fide* salt bridges (Pelletier & Kraut, 1992; I. Jelesarov and H. R. Bosshard, unpublished calculations).

In conclusion, electrostatic attraction may contribute to the free energy of a coiled coil without that specific salt bridges have to form. Electrostatic attraction is proposed to be the major cause for the nearly diffusion-limited rate of association at low ionic strength of the A:B heterodimer. More generally, the findings demonstrate that coupled association and folding of a simple dimeric protein motif can be as fast as the fastest folding observed for small single chain proteins (Alexander et al., 1992; Sosnick et al., 1994; Schindler et al., 1995; Kragelund et al., 1995; Huang & Oas, 1995). It will be interesting to see how such very rapid folding of a dimeric structure motif contributes to the overall kinetics of folding of a more complex dimeric protein.

ACKNOWLEDGMENT

We thank Eberhard Dürr and Wim Koppenol for very helpful comments and discussions.

REFERENCES

Alexander, P., Orban, J., & Bryan, P. (1992) *Biochemistry 31*, 7243−7248.
Bernasconi, C. F. (1976) *Relaxation Kinetics*, Academic Press, New York, pp 76−79.
Betz, S. F., Bryson, J. W., & DeGrado, W. F. (1995) *Curr. Opin. Struct. Biol. 5*, 457−463.
Blond, S., & Goldberg, M. E. (1985) *J. Mol. Biol. 182*, 597−606.
Debye, P., & Hückel, E. (1923) *Phys. Z. 24*, 185−206.
Dill, K. (1985) *Biochemistry 24*, 1501−1504.
Edelhoch, H. (1967) *Biochemistry 6*, 1948−1954.
Eigen, M., & Hammes, G. G. (1963) *Adv. Enzymol. 25*, 1−38.
Ellenberger, T. (1994) *Curr. Opin. Struct. Biol. 4*, 12−21.
Ellenberger, T. E., Brandl, C. J., Struhl, K., & Harrison, S. C. (1992) *Cell 71*, 1223−1237.
Fersht, A. R. (1995) *Proc. Natl. Acad. Sci. U.S.A. 92*, 10869−10873.
Gittelman, M. S., & Matthews, C. R. (1990) *Biochemistry 29*, 7011−7020.
Glover, J. N. M., & Harrison, S. C. (1995) *Nature 373*, 257−261.
Goldberg, M. E. (1985) *Trends Biochem. Sci. 10*, 388−391.

Graddis, T. J., Myszka, D. G., & Chaiken, I. M. (1993) *Biochemistry 32*, 12664−12671.
Hai, T., & Curran, T. (1991) *Proc. Natl. Acad. Sci. U.S.A. 88*, 3720−3724.
Hammes, G. G., & Roberts, P. B. (1969) *J. Am. Chem. Soc. 91*, 1812−1816.
Hodges, R. S., Sodek, J., Smillie, L. B., & Jurasek, L. (1972) *Cold Spring Harbor Symp. Quant. Biol. 37*, 299−310.
Huang, G. S., & Oas, T. G. (1995) *Proc. Natl. Acad. Sci. U.S.A. 92*, 6878−6882.
Hurst, H. C. (1995) in *Protein Profile* (Sheterline, P., Ed.) pp 105−168, Academic Press, London.
Jaenicke, R. (1987) *Prog. Biophys. Mol. Biol. 49*, 117−237.
Jelesarov, I., & Bosshard, H. R. (1996) *J. Mol. Biol. 263*, 344−358.
Junius, F. K., Mackay, J. P., Bubb, W. A., Jensen, S. A., Weiss, A. S., & King, G. F. (1995) *Biochemistry 34*, 6164−6174.
Kohn, W. D., Kay, C. M., & Hodges, R. S. (1995) *Protein Sci. 4*, 237−250.
König, P., & Richmond, T. J. (1993) *J. Mol. Biol. 233*, 139−154.
Koppenol, W. H. (1980) *Biophys. J. 29*, 493−507.
Koppenol, W. H., & Margoliash, E. (1982) *J. Biol. Chem. 257*, 4426−4437.
Kragelund, B. B., Robinson, C. V., Knudsen, J., Dobson, C. M., & Poulsen, F. M. (1995) *Biochemistry 34*, 7217−7224.
Krylov, D., Mikhailenko, I., & Vinson, C. R. (1994) *EMBO J. 13*, 2849−2861.
Landschulz, W. H., Johnson, P. F., & McKnight, S. L. (1988) *Science 240*, 1759−1764.
Lavigne, P., Sönnichsen, F. D., Kay, C. M., & Hodges, R. S. (1996) *Science 268*, 1136−1137.
Lumb, K. J., & Kim, P. S. (1995a) *Biochemistry 34*, 8642−8648.
Lumb, K. J., & Kim, P. S. (1995b) *Science 268*, 436−439.
Lumb, K. J., & Kim, P. S. (1996) *Science 271*, 1137−1138.
Mann, C. J., & Matthews, C. R. (1993) *Biochemistry 32*, 5282−5290.
Marcus, Y. (1994) *Biophys. Chem. 51*, 111−127.
Margoliash, E., & Bosshard, H. R. (1983) *Trends Biochem. Sci. 8*, 316−320.
Milla, M. E., & Sauer, R. T. (1994) *Biochemistry 33*, 1125−1133.
Milla, M. E., Brown, B. M., Waldburger, C. D., & Sauer, R. T. (1995) *Biochemistry 34*, 13914−13919.
Myszka, D. G., & Chaiken, I. M. (1994) *Biochemistry 33*, 2363−2372.
O'Shea, E. K., Rutkowski, R., & Kim, P. S. (1989a) *Science 243*, 538−542.
O'Shea, E. K., Rutkowski, R., Stafford, W. F., III, & Kim, P. S. (1989b) *Science 245*, 646−648.
O'Shea, E. K., Klemm, J. D., Kim, P. S., & Alber, T. (1991) *Science 254*, 539−544.
O'Shea, E. K., Lumb, K. J., & Kim, P. S. (1993) *Curr. Biol. 3*, 658−667.
Ozeki, S., Kato, T., Holtzer, M. E., & Holtzer, A. (1991) *Biopolymers 31*, 957−966.
Pelletier, H., & Kraut, J. (1992) *Science 258*, 1748−1755.
Qian, H. (1994) *Biophys. J. 67*, 349−355.
Robinson, R. A., & Stokes, R. H. (1959) *Electrolyte Solutions*, pp 223−252, Butterworth, London.
Rudolph, R., Fuchs, I., & Jaenicke, R. (1986) *Biochemistry 25*, 1662−1669.
Schindler, T., Herrler, M., Marahiel, M. A., & Schmid, F. X. (1995) *Nat. Struct. Biol. 2*, 663−674.
Schreiber, G., & Fersht, A. R. (1996) *Nat. Struct. Biol. 3*, 427−431.
Schwarz, G. (1965) *J. Mol. Biol. 11*, 64−77
Semisotnov, G. V., Rodionova, N. A., Razgulayev, O. I., Uversky, V. N., Gropas, A. F., & Gilmanshin, R. I. (1991) *Biopolymers 31*, 119−128.
Sosnick, T. R., Mayne, L., Hiller, R., & Englander, S. W. (1994) *Nat. Struct. Biol. 1*, 149−156.
Sosnick, T. R., Jackson, S., Wilk, R. R., Englander, S. W., & DeGrado, W. F. (1996a) *Proteins 24*, 427−432.
Sosnick, T. R., Mayne, L., & Englander, S. W. (1996b) *Proteins 24*, 413−426.
Thomas, R. M., Wendt, H., Zampieri, A., & Bosshard, H. R. (1995) *Prog. Colloid Polym. Sci. 99*, 24−30.
Waldburger, C. D., Jonsson, T., & Sauer, R. T. (1996) *Proc. Natl. Acad. Sci. U.S.A. 93*, 2679−2634.
Wendt, H., Baici, A., & Bosshard, H. R. (1994) *J. Am. Chem. Soc. 116*, 6973−6974.
Wendt, H., Berger, C., Baici, A., Thomas, R. M., & Bosshard, H. R. (1995) *Biochemistry 34*, 4097−4107.
Williams, S., Causgrove, T. P., Gilmanshin, R., Fang, K. S., Callender, R. H., Woodruff, W. H., & Dyer, R. B. (1996) *Biochemistry 35*, 691−697.
Zetina, C. R., & Goldberg, M. E. (1980) *J. Mol. Biol. 137*, 401−414.
Zetina, C. R., & Goldberg, M. E. (1982) *J. Mol. Biol. 157*, 133−148.
Zhou, N. E., Kay, C. M., & Hodges, R. S. (1992) *Biochemistry 31*, 5739−5746.
Zhou, N. E., Kay, C. M., & Hodges, R. S. (1994) *J. Mol. Biol. 237*, 500−512.
Ziegler, M. M., Goldberg, M. E., Chaffotte, A. F., & Baldwin, T. O. (1993) *J. Biol. Chem. 268*, 10760−10765.
Zitzewitz, J. A., Bilsel, O., Luo, J. B., Jones, B. E., & Matthews, C. R. (1995) *Biochemistry 34*, 12812−12819.

BI961672Y